ACS APPLIED MATERIALS & INTERFACES

www.acsami.org

Research Article

Layer-by-Layer Assembly of a Polysaccharide "Armor" on the Cell Surface Enabling the Prophylaxis of Virus Infection

Zhiqiang Nie,[#] Yinghao Li,[#] Xinxin Li, Youqian Xu, Guanyuan Yang, Ming Ke, Xiaohang Qu, Yinhua Qin, Ju Tan, Yonghong Fan,[*] and Chuhong Zhu[*]

Cite This: https://doi.org/10.1021/acsami.2c03442

Read Online

ACCESS | Metrics & More | Article Recommendations | Supporting Information

ABSTRACT: Airborne pathogens, such as the world-spreading severe acute respiratory syndrome coronavirus-2 (SARS-CoV-2), cause global epidemics via transmission through the respiratory pathway. It is of great urgency to develop adequate interventions that can protect individuals against future pandemics. This study presents a nasal spray that forms a polysaccharide "armor" on the cell surface through the layer-by-layer self-assembly (LBL) method to minimize the risk of virus infection. The nasal spray has two separate components: chitosan and alginate. Harnessing the electrostatic interaction, inhaling the two polysaccharides alternatively enables the assembly of a barrier that reduces virus uptake into the cells. The results showed that this approach has no obvious cellular injury and endows cells with the ability to resist the infection of adenovirus and SARS-CoV-2 pseudovirus. Such a method can be a potential preventive strategy for protecting the respiratory tract against multiple viruses, especially the upcoming SARS-CoV-2 variants.

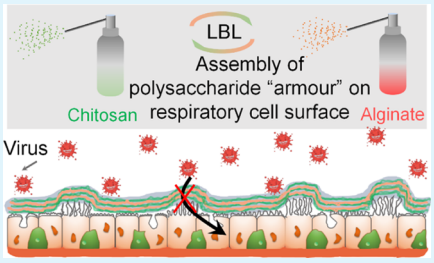

KEYWORDS: *LBL, SARS-CoV-2, chitosan, nasal spray, infection, alginate*

1. INTRODUCTION

The global coronavirus disease 2019 (COVID-19) pandemic has caused about 332 million cases of infection and more than 5 million deaths since it was first reported.[1] Due to its high virulence and contagiousness, it is important to develop adequate management to stop this pandemic. Vaccination and therapeutic drugs are the mainstay strategies used to overcome the outbreak. However, it takes quite a long time from laboratory to patients and often lags behind the pandemics. Despite some specific antiviral drugs and vaccines against COVID-19 that have been used in clinics, which have suppressed the severity of the cases, the spreading of SARS-CoV-2 has not been stamped out at present.[2,3] In addition, the maldistribution of drugs and vaccines among countries, asymptomatic carriers, and mutations of the virus complicates the control of the epidemic.[4] Thus, it is more important to protect individuals from virus infection.

There is definite evidence that inhalation of virus-laden aerosols is a major transmission route for COVID-19.[5] Airborne transmission of the coronaviridae (CoVs) family, including Middle East respiratory syndrome (MERS), SARS, and SARS-CoV-2 viruses, has elicited increasing attention toward the prevention of respiratory infections. Virus-laden droplets and aerosols are generated by infected individuals and transported into the environment. Although most of the droplets (>100 μm) fall to the ground in seconds, the rest may be sprayed to the nearby individuals and inhaled. However, the aerosols (<100 μm) can pervade in the air for many seconds to hours and inhaled by the passerby to initiate a new infection.[6] Model simulations and practice have demonstrated that the masks effectively prevented asymptomatic transmission and reduced COVID-19 infections and mortalities.[7] Wearing of masks provides a critical barrier that not only reduces the exhalation of infectious viruses from the carriers but also protects uninfected individuals from virus-laden aerosols and droplets.[8,9] More recently, some face masks made of antiviral fabrics were developed to increase protection.[10,11] However, the small gaps between the mask and the facial contours result in leakages that substantially decrease the effectiveness of the masks.[12] The efficiency of the masks decreases by 50% when the relative leak area reaches 1% for the aerosols, < 2.5 μm.[13] Wearing masks for a long time makes the material become airtight as caused by excessive moisture, resulting in the inhalation and exhalation of unfiltered virus-laden aerosols around the edges. In addition, the filtration efficacy of airborne virus concentration shows a nonlinear dependence, where the higher virus abundance leads to the lower mask efficacy. Therefore, more effective or additional preventive interventions should be developed to protect individuals in the medical centers that treat COVID-19 patients, airports, and supermarkets.[14]

Received: February 24, 2022
Accepted: May 19, 2022

Scheme 1. Illustration of the Application of the Nasal Spray to form a Polysaccharide "Armor" on the Cell Surface to Reduce Virus Infection

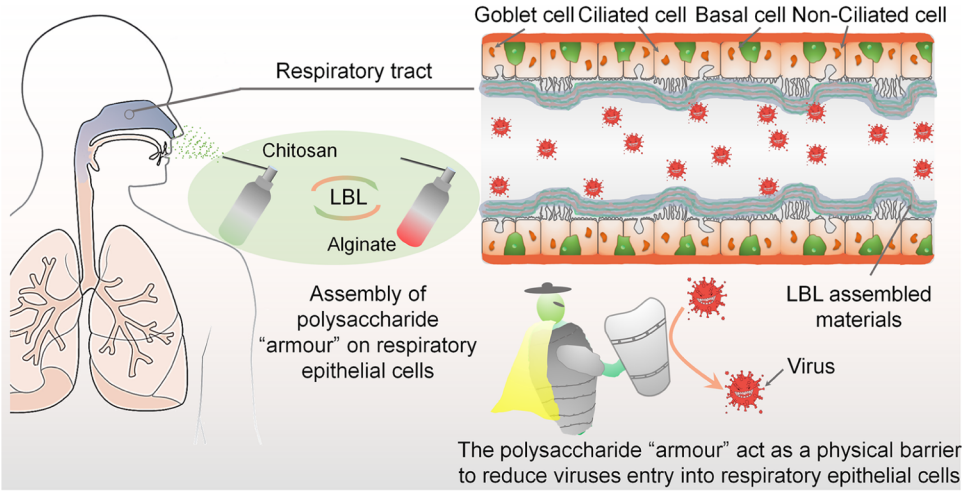

Coronaviruses can adhere to the airway epithelium and then enter the cells once inhaled. Spike proteins on the surface of the coronaviruses can recognize some cell receptors and facilitate virion entry into the host cells.[15] Nasal sprays that can either inactivate the viruses or block its entry into cells are the potent alternatives for preventing the viral spread to the lung or the surrounding people.[16−18] These attempts include nanobodies,[19−21] nanodecoys,[22,23] nanoenzymes,[24] and antiseptics.[25−28] Previous publications have demonstrated that inhalation of angiotensin converting enzyme II (ACE2) nanodecoys derived from human lung spheroid cells (LSCs) can bind and neutralize SARS-CoV-2, protect the host lung cells from infection, and accelerate clearance of SARS-CoV-2 mimics from the lungs.[23] The nanodecoys were found to reside in the lungs for over 72 h post-delivery. More recently, Moakes et al. have developed a composite-based spray that contains algae-isolated carrageenan and gellan polysaccharide. This spray enabled an enhanced surface coverage and prophylaxis of SARS-COV-2.[29] This fully preventive spray allows the entrapment of SARS-COV-2 within a polymeric coating and sterically prevents the virus from entering the cells, as well as inactivating and clearing the virus. These achievements show great advantages of the nasal sprays in fighting COVID-19 and inspiring us to develop more precautions for the upcoming new variants.[30]

In this work, we developed a nasal spray with two separate components, the positively charged chitosan and the negatively charged alginate. Sequential inhalation of these two biomaterials induces the formation of a polysaccharide "armor" on the cell surface through layer-by-layer assembly and blocks virus entry into the cells (Scheme 1). Unlike the normal reported nasal sprays with drugs, antibodies, bioactive proteins, or cellular constituents, our formulation uses Food and Drug Administration (FDA) approved materials that are widely used in clinics. In comparison with the formulations approximate to pharmaceutics, our physical approach is simple and is easily transitioned from the laboratory to the clinic. Moreover, mucociliary clearance should be considered when developing nasal spray therapeutics.[31] The positively charged chitosan has been demonstrated to be an effective absorption enhancer for nasal products, which can be retained in the nasal cavity for extended time periods, thus ensuring the adequate stability of the polysaccharide barrier.[32] Therefore, this layer-by-layer self-assembly (LBL) approach might be more promising in resisting mucociliary clearance compared to the negatively charged xylitol[22] or carrageenan,[29,33] as previously described.

Here, the assembly of chitosan and alginate on the cell surface was explored and optimized, and the preventive effect of the "armor" on virus infection was determined in the presence of adenovirus and SARS-CoV-2 pseudovirus. In addition, the sprayability of the formulations was also assessed. This strategy provides more opportunities for the individuals to fight the emerging SARS-CoV-2 variants.

2. MATERIALS AND METHODS

2.1. Materials. Commercial chitosan hydrochloride (CAS No. 70694-72-3, degree of deacetylation = 90.4%, viscosity (1%) = 71 mPa·s, United States Pharmacopoeia (USP) grade) was purchased from Zhejiang Golden-Shell Pharmaceutical Co., Ltd., China. Sodium alginate (CAS No. 9005-38-3, viscosity (1%) = 520 mPa·s, MW = 80−120 kDa, M/G = 65/35, USP grade) was obtained from Shandong Xiya Reagent Co., Ltd., China. Fluorescein isothiocyanate (FITC) and Cy5-conjugated alginate were synthesized as described in the Supporting Information. Dulbecco's modified Eagle's medium with high glucose (DMEM, Cat No. E600003-0500) and fetal bovine serum (FBS, Cat No. E600001-0500) were purchased from Shanghai Sangon Biotech Co., Ltd., China. Nonessential Amino Acid (NEAA, Cat No. 11140076) cell culture supplement was from Gibco. Minimum essential medium-α (α-MEM, Cat No. SH30265.01) and penicillin−streptomycin (PS, Cat No. SV30010) cell culture supplement were purchased from HyClone. iCell Primary Epithelial Cell Culture System (PECCS, Cat No. PriMed-iCell-001) was obtained from Shanghai iCell Bioscience Inc., China. D-Hanks buffer (Cat No. HA2004Y-2) was from Tianjin Haoyang Biological Manufacture Co., Ltd., China. Dulbecco's phosphate buffered saline (DPBS) was purchased from Shanghai Biochemical Co., Ltd., China (Cat No. D6501). Adenovirus with the enhanced green fluorescent protein reporter gene (pHBAd-EGFP, Cat No. LNAP20022403) was purchased from Shanghai Hanbio Biotechnology Co., Ltd., China. COVID-19-spike protein pseudovirus (nCOV-PV, Cat No. 11906ES50) and FITC-Phalloidin (Cat No. 40735ES75) were obtained from Shanghai Yeasen Biotechnology Co., Ltd., China. Rabbit anti-ACE2 polyclonal antibody (Cat No. bs-1004r) was purchased from Beijing Biosynthesis Biotechnology Co., Ltd., China. Alexa Fluor 568 conjugated goat anti-rabbit IgG (H + L) secondary

https://doi.org/10.1021/acsami.2c03442
ACS Appl. Mater. Interfaces XXXX, XXX, XXX−XXX

antibody (Cat No. A-11011) was from Invitrogen. All of the materials and reagents mentioned in this study were used as received.

2.2. Cell Culture. The human lung adenocarcinoma cell line (CALU3, Cat No. BC1179) was purchased from Chongqing Biospes Biotech Co., Ltd., China, and cultured in MEM medium containing 10% FBS, 1% PS, and 1% NEAA. Human bronchial epithelial cells (HBEpiC, Cat No. CP-H008) were purchased from Wuhan Procell Life Science & Technology Co., Ltd., China, and cultured in PECCS. Human pulmonary alveolar epithelial cells (HPAEpiC, Finetest, Cat No. C799) were obtained from Chongqing Jiukang Medical Research Institute Co., Ltd., China, and cultured in DMEM containing 10% FBS and 1% PS. HEK-293T-ACE2 (293T, Cat No. 41107ES03) cells were obtained from Shanghai Yeasen Biotechnology Co., Ltd., China, and cultured with DMEM medium containing 10% FBS, 1% PS, and 3 μg/mL puromycin. All of the cells were cultured at 37 °C with 5% CO_2 in a humid atmosphere.

2.3. Assembly and Characterization of the Polysaccharide "Armor" on Cells. *2.3.1. LBL Assembly of the Polysaccharide "Armor".* Chitosan hydrochloride and sodium alginate were dissolved in DPBS to form stock solutions (1%, w/v) separately. A working solution was obtained by diluting the stock solution with D-Hank's. In this study, the positively charged chitosan constituent was referred to as C, while the negatively charged alginate constituent was referred to as A. The cells were seeded on poly-L-lysine (PLL)-coated coverslips and cultured for 24 h before use. The LBL self-assembly processes were performed by alternate incubation of the cells with working solutions C and A. Briefly, the cells were washed three times with D-Hank's, followed by incubation with 0.5 mL of C for 4 min. After washing with D-Hank's three times to remove the residual constituents, 0.5 mL of A was added and incubated for another 4 min. The assembly and rinsing procedures were repeated until the desired multilayer coating was obtained.

2.3.2. Scanning Electron Microscopy (SEM) Imaging. The cells were rinsed with DPBS and fixed by 2.5% glutaraldehyde for 12 h, followed by gradient dehydration with ethanol and tert-butyl alcohol. After sputtering with gold for 30 s, the cells were observed under SEM (ZEISS Crossbeam 340).

2.3.3. Flow Cytometry Assay. CALU3 cells were dissociated by 0.25% trypsin to form a single cell suspension in the working solution, and then the LBL self-assembly processes were carried out in centrifuge tubes in accordance with the assembly and rinsing procedures as described above. Subsequently, the cells were collected by centrifugation at 1500 rpm for 3 min and resuspended in DPBS containing 1% FBS to a cell density of 2×10^6 cells/mL. A flow cytometry assay was performed on a BD Accuri C6 Plus instrument.

2.3.4. Confocal Laser Scanning Microscopy (CLSM) Observation. The suspended cells were collected by centrifugation and then fixed with 4% paraformaldehyde for 15 min. The cells were stained with DAPI (10 μg/mL), washed, and then resuspended in DPBS. After mounting on a glass slide using antifade medium (Solarbio, Cat No. S2100), the cells were observed under CLSM (ZEISS, LSM900).

2.3.5. Transmission Electron Microscopy (TEM) Assay. The single cell suspension was centrifuged to form cell masses and fixed with 2.5% glutaraldehyde for 12 h, followed by rinsing with 0.1 M sodium cacodylate buffer (pH = 7.4). Then, the cells were post-fixed with 2% OsO_4 in 0.2 M cacodylate buffer for 1.5 h, dehydrated in graded acetone solutions, permeated with propylene oxide, and embedded in Epon-812. Ultrathin sections (80 nm) of the cells were mounted on 300-mesh grid and then counterstained with uranyl acetate and lead citrate. Finally, the samples were examined with TEM (JEM 1400) with a maximum acceleration voltage of 80 kV.

2.3.6. Zeta Potential Assay. Zeta potential of the suspended single cells was measured on a ζ potential analyzer from Brookhaven Instruments Corporation. All of the measurements were performed at 25 °C. The mean ζ potential was obtained from triplicates.

2.4. Cell Viability Assay. *2.4.1. Live/Dead Staining.* The cell survival was analyzed using a Calcein-AM/EthD-I staining kit (BestBio, Shanghai, China, Cat No. BB-4127). The procedure was carried out in accordance with the manufacture's instructions. Briefly, 2 μL of Calcein-AM and 2 μL of EthD-I were added into 2 mL of DPBS to obtain a working solution first. Then, the cells were washed with DPBS and incubated with 300 μL of staining buffer at 37 °C for 15 min. After washing with DPBS, the cells were observed under an EVOS fluorescence microscope. The cell counts and survival rate were analyzed by Image J software.

2.4.2. Cell Counting Kit-8 (CCK-8) Assay. CALU3 cells were seeded in cell culture plates and cultured for 24 h before use. Then, the cells were treated with working solutions C and A. At predetermined time intervals, the cells were washed with DPBS three times and incubated with a cell culture medium containing 10% CCK-8 reagent (Solarbio, Beijing, China, Cat No. CA1210-500T) at 37 °C for 1 h. A microplate reader (Tecan, Infinite M200 pro) was used to determine the absorbance at 450 nm.

2.4.3. Cytoskeleton Staining. CALU3 cells were dissociated into single cell suspensions, followed by LBL assembly processes. Subsequently, the cells were seeded on coverslips and cultured for a predetermined duration. After washing with DPBS three times, the cells were fixed with 4% paraformaldehyde for 15 min, treated with 0.1% Triton for 30 min, and stained with FITC-conjugated phalloidin (100 nM) for 30 min. Finally, the cell nucleus was counterstained by 4′,6-diamidino-2-phenylindole (DAPI 10 μg/mL), and then the samples were observed under an EVOS fluorescence microscope.

2.5. Virus Transfection. The cells were seeded in 24-well cell culture plates (1×10^5 cells/well) and the assembly procedures were performed. Then, the adenovirus (5 μL, 1×10^5 PFU/mL) or SARS-CoV-2 pseudovirus (1.5 μL, 1×10^6 TU/mL) was added into the medium. After 24 h of incubation, the medium was replaced, and the cells were cultured for another 24 h. The entire virus transfection process was carried out in a cell culture chamber (temperature: 37°C, humidity: 95%, carbon dioxide concentration: 5%). The cells were washed with DPBS and then observed under an EVOS fluorescence microscope. Cells for flow cytometry assay were prepared by seeding 2×10^5 cells/well in a 12-well plate, followed by treating with the virus (5 μL of adenovirus or 3 μL of pseudovirus) after LBL assembly, and then digested into single cell suspension.

2.6. Immunofluorescence Staining. ACE2-positive 293T cells bearing the polysaccharide "armor" were fixed with 4% paraformaldehyde for 15 min and then rinsed with DPBS three times. Next, the cells were blocked with 3% BSA at room temperature for 30 min and incubated with primary antibody to ACE2 (1:200 dilution) at 4 °C in a humid chamber overnight. Then, the cells were washed and visualized with Alexa Fluor 568 conjugated secondary antibody (1:500 dilution). The nuclei were counterstained with DAPI (10 μg/mL). Fluorescence images were acquired by an EVOS fluorescence microscope with fixed acquisition settings to allow qualitative assessment of protein levels. The mean fluorescence intensity was measured by Image J software.

2.7. Sprayability Assay. Chitosan solution (0.02%) was mixed with a red dye, while the alginate solution (0.05%) was mixed with a blue dye. Typical handheld applicators from Jiangsu Hongyuan Plastic Products Co., Ltd. were used to vertically spray flat paper recipients 10 cm away. To simulate the nasal cavity, 4.5 cm × 10 cm paper was rolled up to form a pipe, and chitosan and alginate were alternately sprayed. The sprayed paper was allowed to dry in air and then scanned at 450 DPI (color). Images were analyzed with Image J software.

2.8. Animal Experiments. The animal experiments were carried out in accordance with the Laboratory Animal Administration Rules of China and approved by the Ethics Committee of Third Military Medical University. Adult male SD rats (200 g) were obtained from the Laboratory Animal Center of Third Military Medical University. The rats were randomly assigned into three groups. During anesthesia, 100 μL of chitosan solution (0.02%) was dropped into the nostril. Two minutes later, 100 μL of alginate solution (0.05%) was dropped into the nostril. Chitosan and alginate solutions were alternately inhaled to form the $(CA)_2C$ polysaccharide "armor" in the nasal cavity. In the control group, the rats received the same volume of PBS at each step. Subsequently, 100 μL of adenoviruses (1×10^3 PFU/mL, with enhanced GFP reporter gene) were dropped into the nostril. The rats were fed in separate cages with ad libitum provided

https://doi.org/10.1021/acsami.2c03442
ACS Appl. Mater. Interfaces XXXX, XXX, XXX−XXX

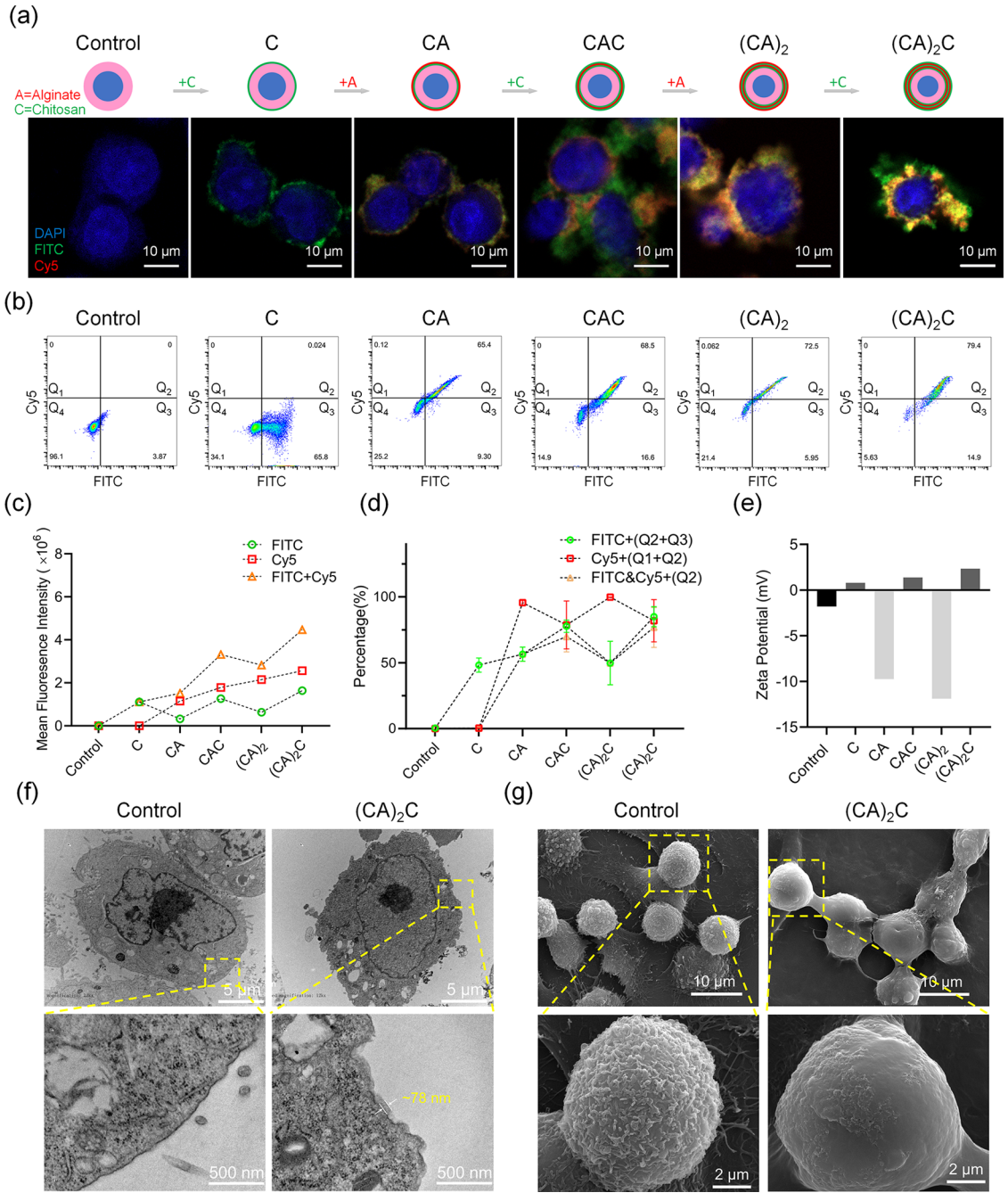

Figure 1. LBL assembly of the polysaccharide "armor" on the CALU3 cell surface. (a) CLSM observation of the FITC-conjugated chitosan and Cy5-conjugated alginate assembly on the CALU3 cell surface. (b) Flow cytometry analysis of the polysaccharide "armor" assembly. (c) Variation of the mean fluorescence intensity during the LBL assembly. (d) Percentage of $FITC^+$, $Cy5^+$, and $FITC\&Cy5^+$ cells obtained from flow cytometry. (e) Zeta potential of the cells from each step. (f) TEM analysis of the cells before and after LBL assembly. (g) Representative SEM images of the cells coated with the polysaccharide "armor".

food and water. Seven days after adenovirus administration, their lungs, tracheas, and nasal mucosas were collected and fixed with 4% paraformaldehyde for 24 h. The tissues were cryosectioned (10 μm) and mounted on glass slides for further evaluation. Some of the slides were stained with DAPI (10 μg/mL) and observed under an EVOS fluorescence microscope. For hematoxylin and eosin (HE) staining, the tissue sections were stained with hematoxylin solution (Servicebio,Wuhan, China, Cat No. G1004) for 4 min and eosin solution (Biosharp,Anhui, China, Cat No. BL703B) for 3 min. Then, the tissue sections were coverslipped with neutral balsam (Origene, Cat No. ZLI-9555) and observed under an OLYMPUS microscope (IX2-SP).

2.9. Statistical Analysis. Data with error bars were calculated from at least three independent tests and presented as mean ± standard deviation (SD). Comparisons between two groups were analyzed using the two-tailed Student's unpaired t-test. P value less than 0.05 was considered to indicate the statistical significance.

3. RESULTS AND DISCUSSION

3.1. Assembly and Characterization of the Polysaccharide "Armor" on the Cell Surface. LBL self-assembly is an ultrathin film fabrication technique of sequential deposition of multilayers of oppositely charged materials.[34]

https://doi.org/10.1021/acsami.2c03442
ACS Appl. Mater. Interfaces XXXX, XXX, XXX−XXX

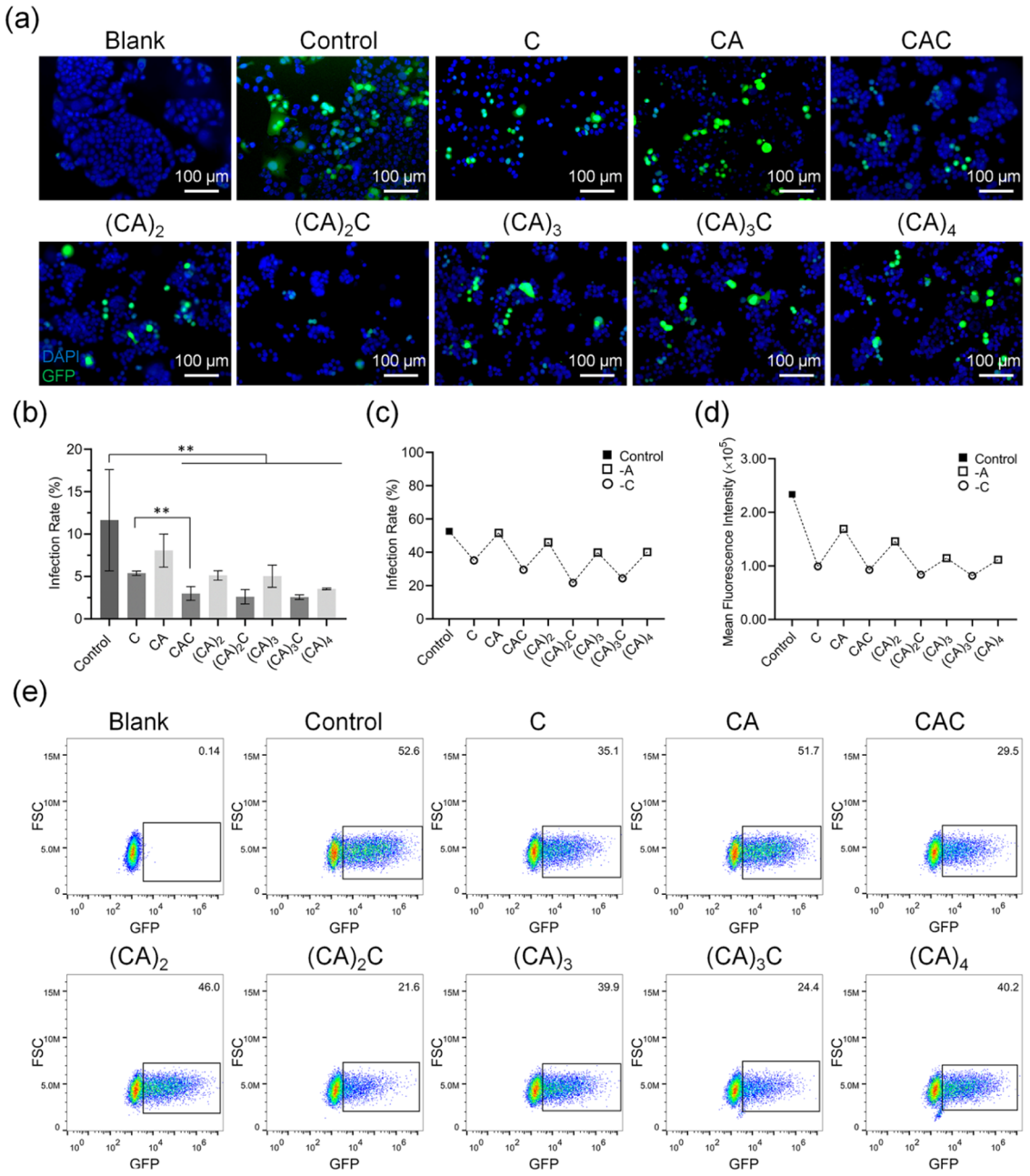

Figure 2. Assembly of the polysaccharide "armor" on the CALU3 cell minimizes the risk of adenovirus infection. (a) Polysaccharide "armor"-coated cells have a lower degree of infection after incubation with adenovirus; the infected cells are marked by GFP. (b) Statistical analysis of the GFP-positive cells based on fluorescence images. (c) Infection rate and (d) mean fluorescence intensity of the cells coated with different layers of polysaccharide as measured by flow cytometry. (e) Flow cytometry results showing the adenovirus infection in polysaccharide-coated cells.

Using biocompatible materials to create a coating on the cell surface enables to protect delicate mammalian cells and impart them with new functionalities.[35−39] In this study, the negatively charged alginate and positively charged chitosan were used to form a polysaccharide "armor" by LBL self-assembly. Both materials are mucoadhesive and have good cytocompatibility at different concentrations (from 0.001 to 0.1%, Figures S1 and S2). Here, 0.02% chitosan and 0.05% alginate were used to fabricate the polysaccharide "armor." To observe the assembly of the two materials on the cell surface, the chitosan was labeled with FITC and the alginate was labeled with Cy5. The negatively charged mammalian cells were assembled with chitosan first, and then checked under CLSM. The result showed the presence of a thin layer of green fluorescence around the cell (Figure 1a). The following alginate assembly resulted in an orange coating rather than forming a separate red shell, indicating a tight interlock between the alginate and chitosan. With the sequential assembly of the two materials, the polysaccharide "armor" on the cell membrane became thicker, leading to gradual increase in the fluorescence intensity. In addition, flow cytometry was used to analyze the assembly processes. After treatment with chitosan, 65.8% of the cells were FITC-positive (Figure 1b). Adsorption of alginate led to 65.4% FITC&CY5$^+$-positive cells. The mean fluorescence intensity and the percentage of FITC&CY5$^+$-positive cells gradually increased with the LBL assembly processes (Figure 1c). Finally, about 79.4% cells were FITC&CY5$^+$-positive, while 94.3% cells were FITC-positive,

https://doi.org/10.1021/acsami.2c03442
ACS Appl. Mater. Interfaces XXXX, XXX, XXX−XXX

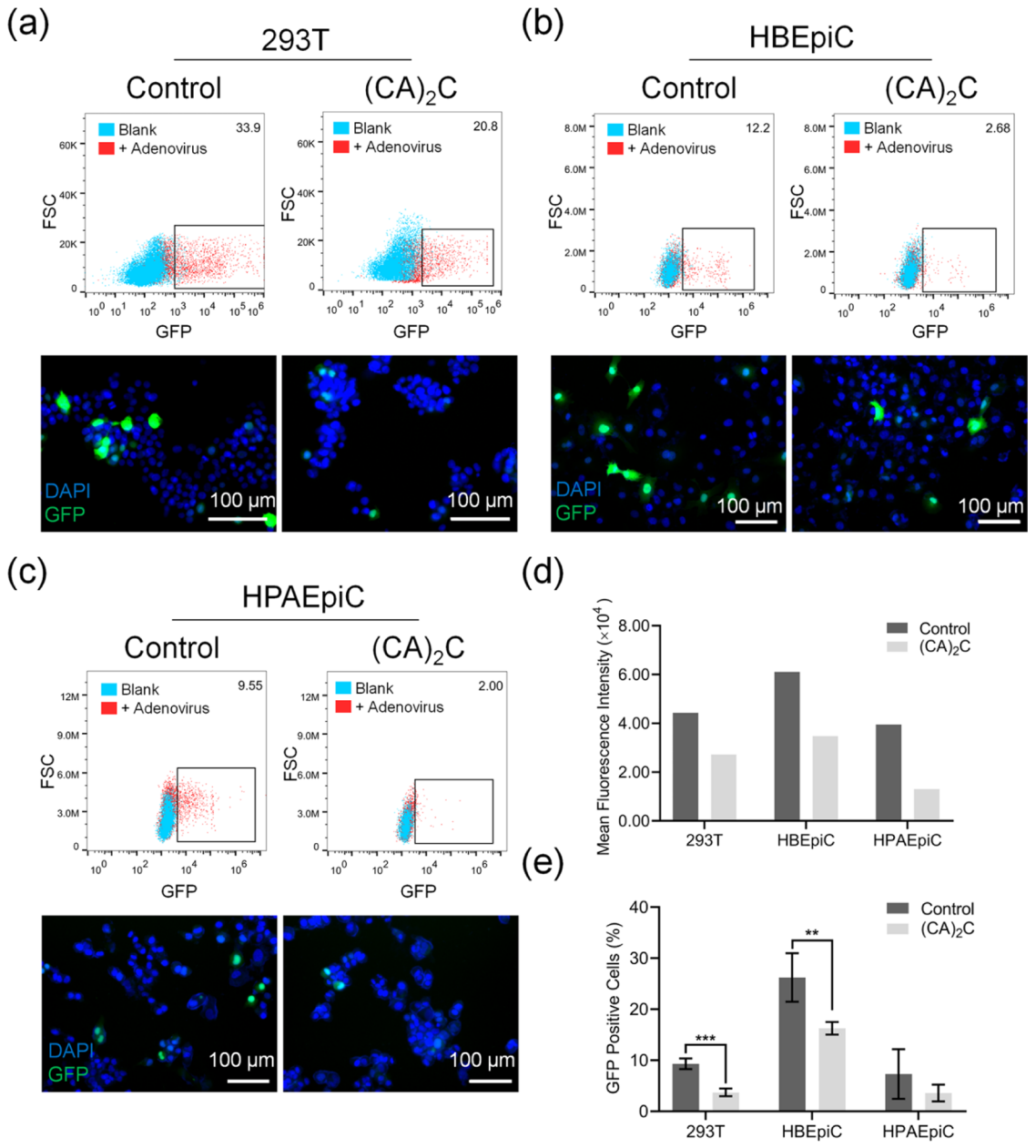

Figure 3. $(CA)_2C$ assembly reduces adenovirus infection in 293T, HPAEpiC, and HBEpiC. Flow cytometry assay and fluorescent observation of adenovirus infection in (a) 293T, (b) HPAEpiC, and (c) HBEpiC. (d) Mean fluorescence intensity of the cells after infection with adenovirus. (e) Proportion of GFP-positive cells calculated from fluorescence images (data are presented as mean ± SD, $*p < 0.05$, $**p < 0.01$, $***p < 0.001$).

indicating that most of the cells were coated with the polysaccharide "armor" (Figure 1d).

The change of ζ potential of the cells was also checked and the results are shown in Figure 1e. The untreated cells were negatively charged but gained positive charges after coating with chitosan. Assembly with alginate led to the reduction of the ζ potential of the cells to below zero. Sequential deposition of chitosan and alginate resulted in the oscillation of the ζ potential between negative and positive. The "armor" was also confirmed by TEM. Compared with the untreated group, the cells in the $(CA)_2C$ group were encapsulated by the material as shown in Figure 1f. The polysaccharide shell was intact and the thickness was measured to be about 78 nm. In addition, coating with the polysaccharide "armor" yielded a smoother cell surface as observed by SEM (Figure 1g). Taken together, our data demonstrated the successful LBL self-assembly of chitosan and alginate on the cell surface.

3.2. Polysaccharide "Armor" Interferes with the Virus Transferring into the Cells. To evaluate the ability of the polysaccharide "armor" bearing CALU3 cells to prevent virus infection, the adenovirus with the GFP reporter gene was used for *in vitro* transfection of the cells. The influence of different polysaccharide layers on the adenovirus infection was also investigated. Fluorescence microscopy and flow cytometry data showed that the polysaccharide-coated cells were able to suppress the virus infection (Figure 2). However, the outermost layer of the polysaccharide assembly had the highest impact on inhibiting virus infection. In addition, the outermost shell of chitosan showed greater suppression of the adenovirus infection in comparison with that of alginate according to the proportion of GFP-positive cells (Figure

https://doi.org/10.1021/acsami.2c03442
ACS Appl. Mater. Interfaces XXXX, XXX, XXX−XXX

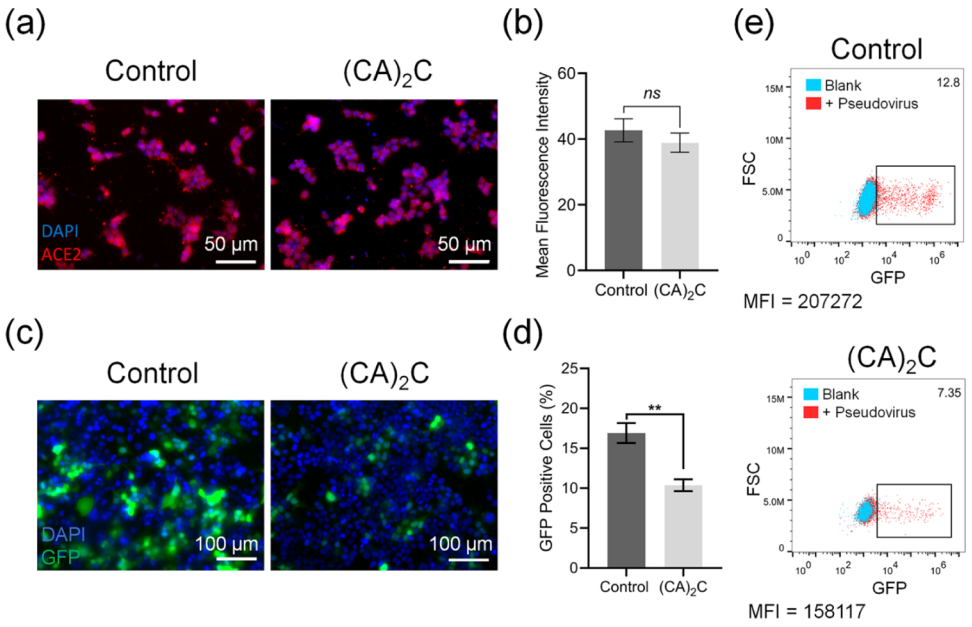

Figure 4. Coating the ACE2-positive 293T cells with $(CA)_2C$ polysaccharide "armor" inhibits uptake of SARS-CoV-2 pseudovirus. (a) Immunofluorescence staining of ACE2 before and after $(CA)_2C$ assembly. (b) Mean fluorescence intensity of ACE2 in the cells. (c) Fluorescence images of pseudovirus infection in the 293T cells. (d) Statistical analysis of GFP-positive cells in fluorescence images. (e) Flow cytometry assay of the pseudovirus infection; MFI: mean fluorescence intensity (data are presented as mean ± SD, ns: not statistically different, $*p < 0.05$, $**p < 0.01$, $***p < 0.001$).

2a,b). The anti-infection property of the cells increased with the chitosan assembly and reached its maximum in $(CA)_2C$. The infection rate of CALU3 decreased to 35.1% after assembly of one chitosan layer, while the rate of infection after CAC assembly was 29.5%. The anti-infection property of the cells increased with the chitosan assembly and reached its maximum in $(CA)_2C$. The infection rate decreased to 21.6% compared to 52.6% in the untreated control (Figure 2c). There was similar tendency in the mean fluorescence intensity as shown in Figure 2d. Further assembly of chitosan and alginate on $(CA)_2C$ did not improve the infection tolerance (Figure 2e). Chitosan, alginate, and their derivatives have been reported to exhibit direct antiviral activity.[40−42] However, our results showed that the chitosan assembly significantly reduced adenovirus infection, but the assembly of alginate did no effort in increasing the protective effect. Thus, it is reasonable to infer that the chitosan played a key role in preventing cells from infection in the present study. According to the previously published work from another group,[43] our polysaccharide "armor" might act as a barrier either inactivating the virus by chitosan or forming steric hindrance at the cell surface in reducing virus entry into cells.

Based on the adenovirus infection in CALU3 cells, $(CA)_2C$ was selected as the optimal pattern to assemble on other kinds of cells. As expected, 293T cells coated with $(CA)_2C$ had significantly reduced adenovirus infection, where the infection rate decreased from 33.9 to 20.8% as determined by flow cytometry (Figure 3a). The percentage of GFP-positive 293T cells was calculated and the result showed that (9.3±1.0)% of 293T cells were GFP-positive in the control group, which decreased to (3.7±0.8)% in the $(CA)_2C$ group. Epithelial cells are the major cell types in the airways and act as a defensive barrier against virus infection.[44] Respiratory epithelial cells line the interface of the external environment and the internal milieu, making it a major target of the inhaled virus.[45] Most of the highly contagious viruses, including SARS-CoV-2, are first transmitted through the airway epithelial cells.[44,46] Thus, the infection of adenovirus was also analyzed in $(CA)_2C$-bearing HBEpiC and HPAEpiC. As shown in Figure 3b,c, coating HBEpiC and HPAEpiC with the $(CA)_2C$ polysaccharide "armor" resulted in a lower infection rate than in the untreated control group as measured by flow cytometry (HBEpiC: 12.2 vs 2.7%, HPAEpiC: 9.6 vs 2.0%). In addition, the mean fluorescence intensity calculated from flow cytometry and the proportion of GFP-positive cells observed by fluorescence microscopy also showed that $(CA)_2C$ gave sufficient cells from infection (Figure 3d,e).

Next, the ability of the polysaccharide "armor"-coated cells to prevent SARS-CoV-2 infection was assessed using an ACE2-positive 293T cell line and SARS-CoV-2 pseudovirus with the GFP reporter gene. Immunofluorescence staining showed that LBL assembly of the polysaccharide coating on the cell surface did not affect the ACE2 expression (Figure 4a,b). Less infected cells (GFP-positive) were observed in the $(CA)_2C$ group compared with the control (Figure 4c,d). Moreover, a flow cytometry assay was performed to determine the pseudovirus infection (Figure 4e). The proportion of GFP-positive cells and the mean fluorescence intensity were decreased in the presence of the polysaccharide coating.

3.3. Polysaccharide "Armor" Does Not Affect the Cell Viability. In practice, the polysaccharide "armor" directly forms on the nasal mucosa lining the epithelium cells. Assembly of the polysaccharide "armor" should not cause any damage to the cells. The live/dead staining assay was carried out to evaluate the influence of the polysaccharide "armor" on cell survival. The living cells were stained green by Calcein-AM, while the dead cells were stained red by EthD-1. The result showed that the $(CA)_2C$ coating did not affect cell growth as shown in the fluorescence images (Figure 5a). Very few dead cells could be seen both in the untreated group and the $(CA)_2C$ group. The cell numbers and cell survival rate were calculated and showed that there was no significant

https://doi.org/10.1021/acsami.2c03442
ACS Appl. Mater. Interfaces XXXX, XXX, XXX−XXX

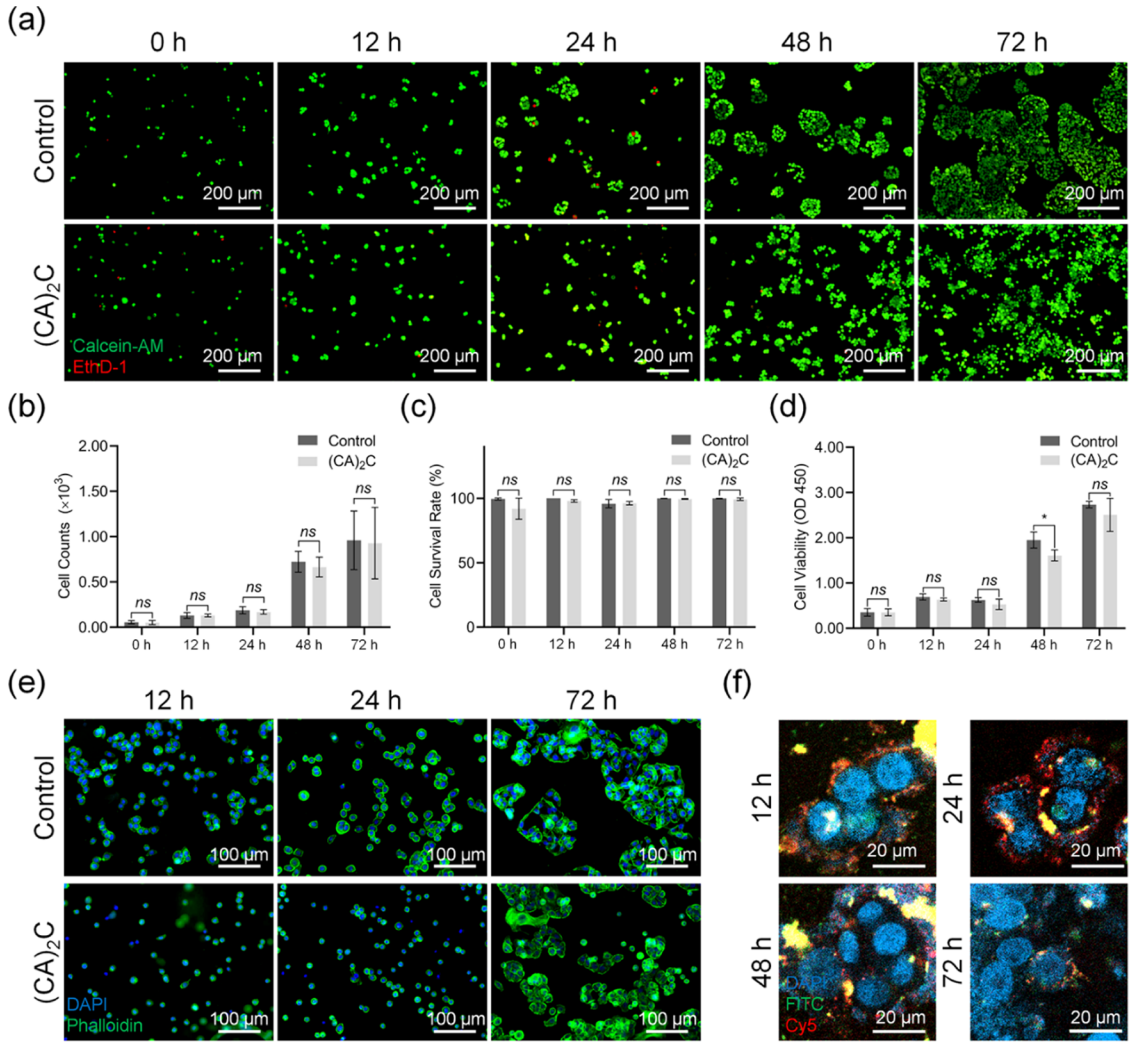

Figure 5. Cell viability assay after coating with the polysaccharide "armor." (a) Live/dead staining of CALU3 cells after LBL assembly; the live cells were stained green with Calcein-AM and the dead cells were stained red with EthD-1. (b) Statistical analysis of live cells as determined from fluorescence images. (c) Comparison of cell survival rate before and after LBL assembly. (d) CCK-8 analysis: data were collected with the absorbance at 450 nm. (e) Cell adhesion and spreading after coating with the polysaccharide "armor"; LBL assembly was performed before cell seeding and the cytoskeleton was stained with FITC-conjugated phalloidin. (f) Stability of the polysaccharide "armor" after culture for 12, 24, 48, and 72 h (data are presented as mean ± SD, ns: not statistically different, $*p < 0.05$).

difference between the control group and the $(CA)_2C$ group (Figure 5b,c). In addition, the cell viability was also measured using a CCK-8 kit. The result indicated a significant proliferation of the cells after 24 h of incubation, and only a very small difference in the CCK-8 value was observed between the control group and the $(CA)_2C$ group (Figure 5d). To evaluate the effect of the polysaccharide "armor" on cell adhesion and spreading, the cells were digested to form a single cell suspension and then reseeded after being coated with the material. As shown in Figure 5e, $(CA)_2C$ coating did not affect cell adhesion but suppressed cell spreading in the first 12 and 24 h. After 72 h of incubation, the cells in the $(CA)_2C$ group and the control group were able to spread. In addition, the durability of the polysaccharide "armor" was determined by tracking the fluorescence decay on the cell surface. Notably, the fluorescence of the polysaccharide decreased markedly after 48 h, indicating that the polysaccharide "armor" may protect the cell from virus infection for more than 2 days (Figure 5f). In general, assembly of the polysaccharide "armor" on the cell surface did not significantly affect cell growth and could provide protection in a long period of time.

3.4. Sprayability of Polysaccharide Formulations. To evaluate the sprayability of the polysaccharide formulations, the chitosan solution and alginate solution were loaded in two simple manual spray pumps separately. The spray distributions on flat paper recipients and tubular paper recipients are shown in Figure 6a,b. As shown in Figure 6c, the polysaccharide solution formed a uniform spray after spurting from the pump aperture. Moreover, the spray of chitosan and alginate formed a homogeneous layer on the flat paper recipients (Figure 6d). Following the increasing spraying times, the cover area of the polysaccharide coating became larger (Figure 6e). The cover area of $(CA)_2C$ reached 57.7 cm^2 as measured from the paper recipients, which exceeded 3/4 of the unilateral nasal cavity.[47] Furthermore, a 4.5 cm × 10 cm paper was rolled up to form a pipe to simulate the tubular structure of the nasal cavity. The chitosan and alginate formulations were alternatively sprayed into the pipe from the orifice. The results showed that the spray covered a large area in the tubular nasal simulator

https://doi.org/10.1021/acsami.2c03442
ACS Appl. Mater. Interfaces XXXX, XXX, XXX−XXX

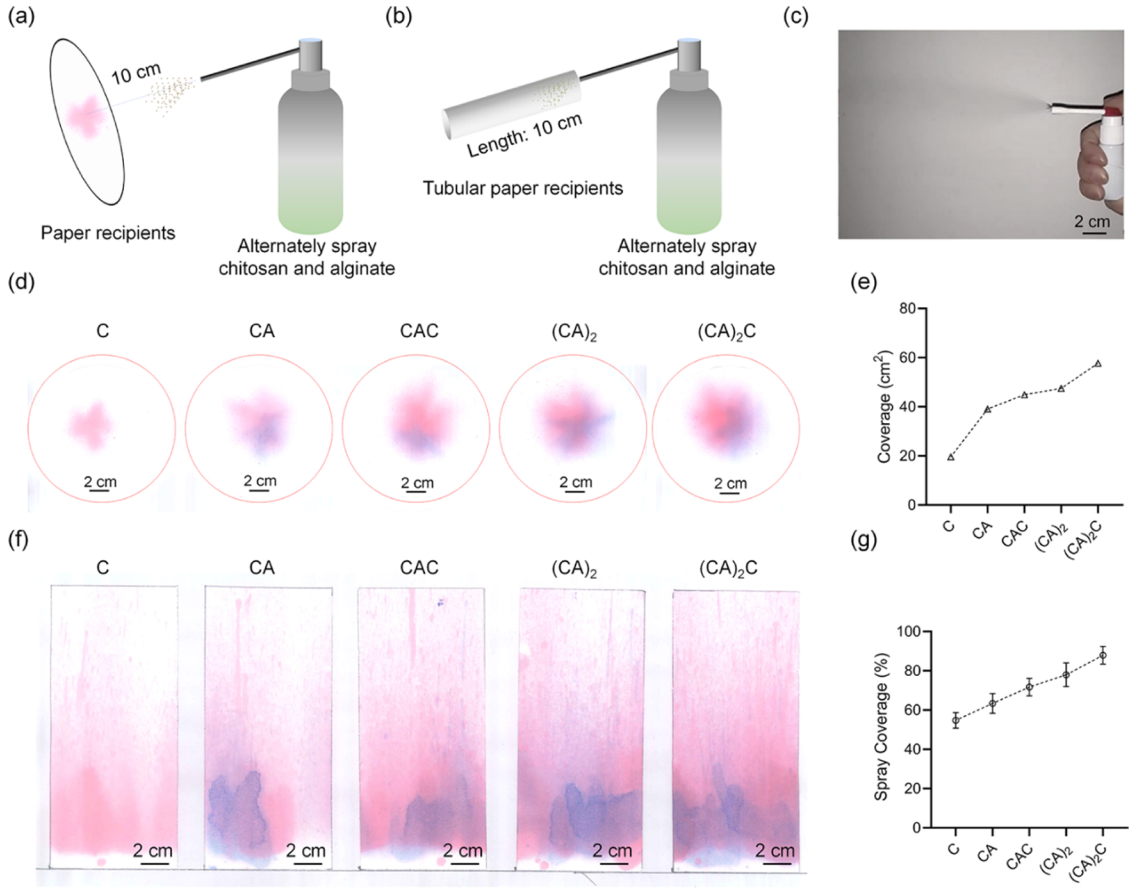

Figure 6. Sprayability of polysaccharide formulations demonstrates the application potential of the approach. The polysaccharide formulations were bottled in handheld applicators and their sprayability was evaluated though two experimental regimens: (a) Vertically spraying flat paper recipients 10 cm away and (b) spraying tubular paper recipients from the orifice. (c) Representative image of the spray formation when the polysaccharide solution was spurted from the applicator. (d) Typical images of spray deposition on the flat paper recipients. (e) Increasing cover area after alternate spraying of the formulations. (f) Alternately sprayed polysaccharide formulation formed an extensive coverage in the tubular nasal simulator. (g) Statistical analysis of spray coverage of the polysaccharide "armor" in the nasal simulator (data are presented as the mean ± SD).

(Figure 6f). The coverage ratio of the polysaccharide "armor" reached up to 87.9% in $(CA)_2C$ (Figure 6g). Chitosan or alginate was sprayed only once in each step of the assembly. It is inferred that multiple sprays will create a homogeneous coating and larger coverage area, which may result in a better anti-infection effect. The sprayability of the polysaccharide formulations revealed that the nasal spray may be a potential intervention for protecting individuals against virus infection.

3.5. Wearing the Polysaccharide "Armor" Reduces Adenovirus Infection in SD Rats. Finally, the protective effects of the polysaccharide "armor" on virus infection were explored using a rat model. Adenoviruses with the GFP reporter gene were used as the model viruses. To mimic the virus infection under personal protection in daily situations, the SD rats in the experimental group were allowed to wear the polysaccharide "armor" before receiving adenovirus (Figure 7a). The rats were fed for 7 days, and then their lungs, trachea, and nasal mucosa were collected and analyzed. Results showed that mock-infected rats and those wearing the protective polysaccharide "armor" exhibited normal histology. However, marked lung inflammation and airway epithelial responses were observed in rats of the unprotected control. The digital images showed an obvious edema after slight hemorrhage in the lungs of unprotected rats (Figure 7b). Multifocal regions of inflammation and consolidation were also observed in the lungs from unprotected group, showing the strong evidence of adenoviral pneumonia.[23,48] Meanwhile, a large number of GFP-positive cells were found in the lung tissue from unprotected rats. In comparison, there was no significant difference in morphology and color of the lungs between the experimental group and the normal control. No instances of lung injury, inflammatory cell infiltration, and GFP-positive cells could be observed in both the mock-infected rats and polysaccharide "armor" protected rats. The HE staining of nasal mucosa revealed an intact mucous membrane in all of the three groups, but a remarkable GFP-positive cell lining was observed in the nasal cavity of the unprotected rats (Figure 7c). In addition, remodeling of airway epithelia, infiltration of inflammatory cells, cell sloughing, and mucous cell metaplasia were noted in the trachea of unprotected rats, indicating marked epithelial differentiation and/or injury caused by virus infection (Figure 7d).[49] There was no significant difference in the HE staining of the trachea between the normal group and the experimental group. Even though there was a possibility of infection in the trachea of unprotected rats, no GFP-positive epithelial cells were found in the fluorescence image (note that some cells with green fluorescence were observed in the subepithelial layer in all of the three groups, indicating false GFP-positive cells). This might be attributed to the apoptosis or cytolysis caused by virus infection in which the GFP-positive

https://doi.org/10.1021/acsami.2c03442
ACS Appl. Mater. Interfaces XXXX, XXX, XXX−XXX

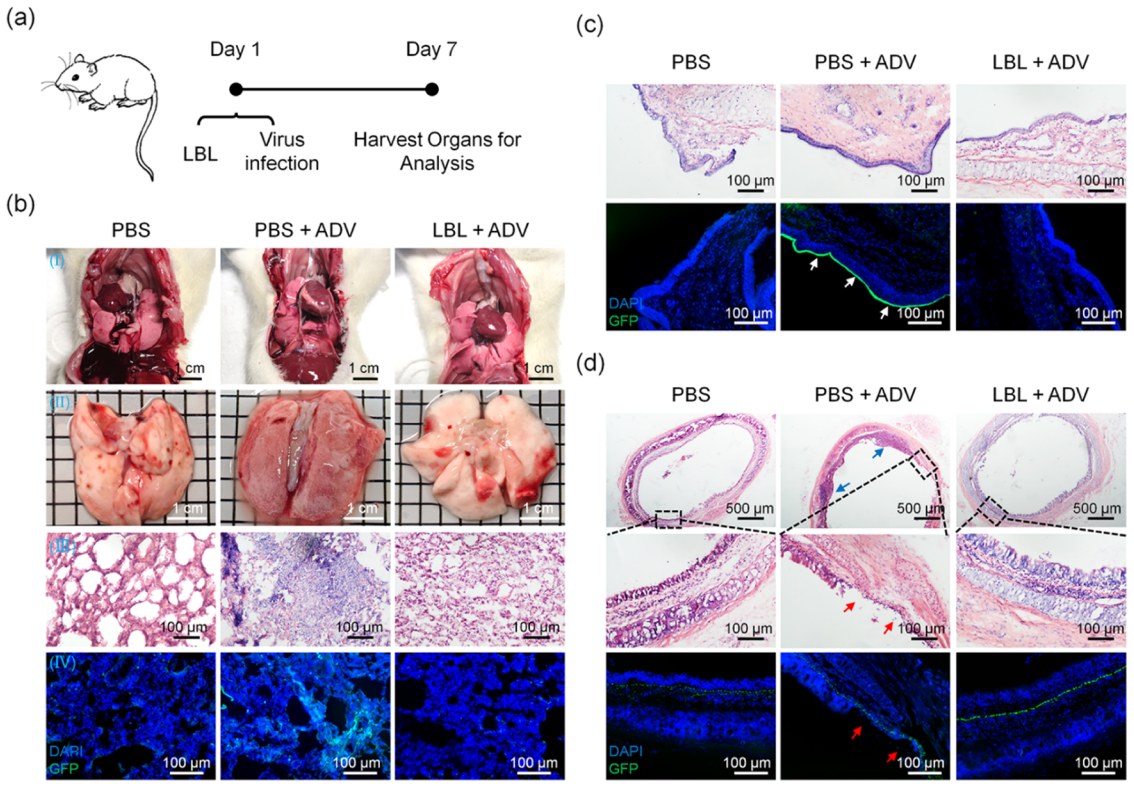

Figure 7. Polysaccharide "armor" reduces adenovirus infection in SD rats. (a) Schematic showing the design of the animal study. (b) Representative images of lung tissues from SD rats after various treatments (I) lungs in the thorax, (II) lungs collected after rinsing with saline, (III) H&E images of fixed lung tissues, (IV) GFP observation of the cryosectioned lung tissues. (c) H&E staining and GFP observation of the nasal mucosa; white arrows indicate the infected mucosa. (d) H&E staining and GFP observation of the trachea; the blue arrows show the remodeling of the airway epithelia and mucous cell metaplasia, and the red arrows indicate sloughing of the epithelium.

cells fell off the epithelia and were cleared from the trachea to limit the replication and spread of virus.[50−52] Taken together, these results demonstrate that assembly of the polysaccharide "armor" in the respiratory tract effectively protected the host from adenovirus infection.

4. CONCLUSIONS

Numerous pathogens exist in the air, such as coronaviruses, adenoviruses, influenza viruses, and respiratory syncytial viruses, spreading in the form of droplets and aerosols. The primary transmission mode for most of the airborne pathogens is their deposition and invasion in the respiratory tract. This implies that prevention of the entry of airborne pathogens into respiratory epithelial cells is important for avoiding infections. This study demonstrates that the LBL assembly of a polysaccharide "armor" using oppositely charged chitosan and alginate on the cell surface can act as a barrier to reduce the risk of virus infection. Assembly of the polysaccharide "armor" had only a negligible effect on cell growth and offered long-term protection against viral infection. Nasal spray made from the two polysaccharides showed good sprayability, indicating that it can be used as a single or additional preventive intervention to extinguish the COVID-19 pandemic.

■ ASSOCIATED CONTENT

Supporting Information

The Supporting Information is available free of charge at https://pubs.acs.org/doi/10.1021/acsami.2c03442.

Synthesis of FITC-conjugated chitosan and Cy5-conjugated alginate; cell viability assay using a CCK-8 kit in the presence of different alginate concentrations (Figure S1); and cell viability assay using a CCK-8 kit in the presence of different chitosan concentrations (Figure S2) (PDF)

■ AUTHOR INFORMATION

Corresponding Authors

Yonghong Fan − *Department of Anatomy, National and Regional Engineering Laboratory of Tissue Engineering, State and Local Joint Engineering Laboratory for Vascular Implants, Key Lab for Biomechanics and Tissue Engineering of Chongqing, Third Military Medical University, Chongqing 400038, China*; Email: yhfan@foxmail.com

Chuhong Zhu − *Department of Anatomy, National and Regional Engineering Laboratory of Tissue Engineering, State and Local Joint Engineering Laboratory for Vascular Implants, Key Lab for Biomechanics and Tissue Engineering of Chongqing, Third Military Medical University, Chongqing 400038, China; State Key Laboratory of Primate Biomedical Research, Institute of Primate Translational Medicine, Kunming University of Science and Technology, Kunming 650500, China; State Key Laboratory of Trauma, Burn and Combined Injury, Chongqing 400038, China*; orcid.org/0000-0002-4214-1800; Email: zhuch99@tmmu.edu.cn

Authors

Zhiqiang Nie − *Department of Anatomy, National and Regional Engineering Laboratory of Tissue Engineering, State*

https://doi.org/10.1021/acsami.2c03442
ACS Appl. Mater. Interfaces XXXX, XXX, XXX−XXX

and Local Joint Engineering Laboratory for Vascular Implants, Key Lab for Biomechanics and Tissue Engineering of Chongqing, Third Military Medical University, Chongqing 400038, China

Yinghao Li − *Department of Anatomy, National and Regional Engineering Laboratory of Tissue Engineering, State and Local Joint Engineering Laboratory for Vascular Implants, Key Lab for Biomechanics and Tissue Engineering of Chongqing, Third Military Medical University, Chongqing 400038, China; Chongqing Institute of Zhong Zhi Yi Gu, Chongqing 400030, China*

Xinxin Li − *State Key Laboratory of Primate Biomedical Research, Institute of Primate Translational Medicine, Kunming University of Science and Technology, Kunming 650500, China*

Youqian Xu − *Department of Anatomy, National and Regional Engineering Laboratory of Tissue Engineering, State and Local Joint Engineering Laboratory for Vascular Implants, Key Lab for Biomechanics and Tissue Engineering of Chongqing, Third Military Medical University, Chongqing 400038, China*

Guanyuan Yang − *Department of Anatomy, National and Regional Engineering Laboratory of Tissue Engineering, State and Local Joint Engineering Laboratory for Vascular Implants, Key Lab for Biomechanics and Tissue Engineering of Chongqing, Third Military Medical University, Chongqing 400038, China*

Ming Ke − *Department of Anatomy, National and Regional Engineering Laboratory of Tissue Engineering, State and Local Joint Engineering Laboratory for Vascular Implants, Key Lab for Biomechanics and Tissue Engineering of Chongqing, Third Military Medical University, Chongqing 400038, China*

Xiaohang Qu − *Department of Anatomy, National and Regional Engineering Laboratory of Tissue Engineering, State and Local Joint Engineering Laboratory for Vascular Implants, Key Lab for Biomechanics and Tissue Engineering of Chongqing, Third Military Medical University, Chongqing 400038, China*

Yinhua Qin − *Department of Anatomy, National and Regional Engineering Laboratory of Tissue Engineering, State and Local Joint Engineering Laboratory for Vascular Implants, Key Lab for Biomechanics and Tissue Engineering of Chongqing, Third Military Medical University, Chongqing 400038, China*

Ju Tan − *Department of Anatomy, National and Regional Engineering Laboratory of Tissue Engineering, State and Local Joint Engineering Laboratory for Vascular Implants, Key Lab for Biomechanics and Tissue Engineering of Chongqing, Third Military Medical University, Chongqing 400038, China*

Complete contact information is available at: https://pubs.acs.org/10.1021/acsami.2c03442

Author Contributions

[#]Z.N. and Y.L. contributed equally to this work.

Notes

The authors declare no competing financial interest.

■ ACKNOWLEDGMENTS

This work was sponsored by the Key projects of the National Natural Science Foundation of China (81830055), the National Science Fund for Distinguished Young Scholars (No. 31625011), and the Special Project for Combating COVID-19 from the State Key Laboratory of Trauma, Burn and Combined Injury.

■ ABBREVIATIONS

ACE2, angiotensin converting enzyme II
CALU3, human lung adenocarcinoma cell line
CAS, chemical abstracts service
CAT, catalogue
CCK-8, cell counting kit-8
CLSM, confocal laser scanning microscopy
Co., Ltd, company limited
COVID-19, coronavirus disease 2019
CoVs, coronaviridae
DAPI, 4′,6-diamidino-2-phenylindole
DMEM, Dulbecco's modified Eagle's medium
DPBS, Dulbecco's phosphate buffered saline
DPI, dots per inch
FBS, fetal bovine serum
FDA, food and drug administration
FITC, fluorescein isothiocyanate
HBEpiC, human bronchial epithelial cells
HEK-293T-ACE2, human embryonic kidney 293T ACE2 overexpress
HPAEpiC, human pulmonary alveolar epithelial cells
LSCs, lung spheroid cells
MERS, middle east respiratory syndrome
MOF, metal-organic framework
nCOV-PV, COVID-19-spike protein pseudovirus
NEAA, nonessential amino acids
NPs, nanoparticles
PECCS, primary epithelial cell culture system
pHBAd-EGFP, adenovirus with enhanced green fluorescent protein reporter gene
PLL, poly-L-lysine
PS, penicillin−streptomycin
RBCs, red blood cells
SARS-CoV-2, severe acute respiratory syndrome coronavirus-2
SEM, scanning electron microscope
TEM, transmission electron microscope
USP, United States pharmacopoeia
α-MEM, minimum essential medium-α

■ REFERENCES

(1) WHO Coronavirus Disease (Covid-19) Pandemic. https://www.who.int/emergencies/diseases/novel-coronavirus-2019 (accessed Jan 19, 2019).

(2) Briz-Redón, Á.; Serrano-Aroca, A. On the Association between Covid-19 Vaccination Levels and Incidence and Lethality Rates at a Regional Scale in Spain. *Stoch. Environ. Res. Risk Assess.* **2022**, 1−8.

(3) Margiotti, K.; Fabiani, M.; Mesoraca, A.; Giorlandino, C. Survey of Fully Vaccinated Anti-Covid 19 People from June to November 2021: Single Italian Center Study. *J. Med. Virol.* **2022**, *94*, 2919−2920.

(4) Rasmussen, A. L.; Popescu, S. V. Sars-Cov-2 Transmission without Symptoms. *Science* **2021**, *371*, 1206−1207.

(5) Prather, K. A.; Marr, L. C.; Schooley, R. T.; McDiarmid, M. A.; Wilson, M. E.; Milton, D. K. Airborne Transmission of Sars-Cov-2. *Science* **2020**, *370*, 303−304.

(6) Wang, C. C.; Prather, K. A.; Sznitman, J.; Jimenez, J. L.; Lakdawala, S. S.; Tufekci, Z.; Marr, L. C. Airborne Transmission of Respiratory Viruses. *Science* **2021**, *373*, No. eabd9149.

(7) Eikenberry, S. E.; Mancuso, M.; Iboi, E.; Phan, T.; Eikenberry, K.; Kuang, Y.; Kostelich, E.; Gumel, A. B. To Mask or Not to Mask: Modeling the Potential for Face Mask Use by the General Public to Curtail the Covid-19 Pandemic. *Infect. Dis. Modell.* **2020**, *5*, 293−308.
(8) Prather, K. A.; Wang, C. C.; Schooley, R. T. Reducing Transmission of Sars-Cov-2. *Science* **2020**, *368*, 1422−1424.
(9) Leung, N. H. L.; Chu, D. K. W.; Shiu, E. Y. C.; Chan, K. H.; McDevitt, J. J.; Hau, B. J. P.; Yen, H. L.; Li, Y.; Ip, D. K. M.; Peiris, J. S. M.; Seto, W. H.; Leung, G. M.; Milton, D. K.; Cowling, B. J. Respiratory Virus Shedding in Exhaled Breath and Efficacy of Face Masks. *Nat. Med.* **2020**, *26*, 676−680.
(10) Seidi, F.; Deng, C.; Zhong, Y.; Liu, Y.; Huang, Y.; Li, C.; Xiao, H. Functionalized Masks: Powerful Materials against Covid-19 and Future Pandemics. *Small* **2021**, *17*, No. e2102453.
(11) Tuñón-Molina, A.; Takayama, K.; Redwan, E. M.; Uversky, V. N.; Andres, J.; Serrano-Aroca, A. Protective Face Masks: Current Status and Future Trends. *ACS Appl. Mater. Interfaces* **2021**, *13*, 56725−56751.
(12) Konda, A.; Prakash, A.; Moss, G. A.; Schmoldt, M.; Grant, G. D.; Guha, S. Aerosol Filtration Efficiency of Common Fabrics Used in Respiratory Cloth Masks. *ACS Nano* **2020**, *14*, 6339−6347.
(13) Drewnick, F.; Pikmann, J.; Fachinger, F.; Moormann, L.; Sprang, F.; Borrmann, S. Aerosol Filtration Efficiency of Household Materials for Homemade Face Masks: Influence of Material Properties, Particle Size, Particle Electrical Charge, Face Velocity, and Leaks. *Aerosol Sci. Technol.* **2021**, *55*, 63−79.
(14) Cheng, Y.; Ma, N.; Witt, C.; Rapp, S.; Wild, P. S.; Andreae, M. O.; Pöschl, U.; Su, H. Face Masks Effectively Limit the Probability of Sars-Cov-2 Transmission. *Science* **2021**, *372*, 1439−1443.
(15) Winkler, E. S.; Bailey, A. L.; Kafai, N. M.; Nair, S.; McCune, B. T.; Yu, J.; Fox, J. M.; Chen, R. E.; Earnest, J. T.; Keeler, S. P.; Ritter, J. H.; Kang, L. I.; Dort, S.; Robichaud, A.; Head, R.; Holtzman, M. J.; Diamond, M. S. Sars-Cov-2 Infection of Human Ace2-Transgenic Mice Causes Severe Lung Inflammation and Impaired Function. *Nat. Immunol.* **2020**, *21*, 1327−1335.
(16) Xi, J.; Lei, L. R.; Zouzas, W.; April Si, X. Nasally Inhaled Therapeutics and Vaccination for Covid-19: Developments and Challenges. *MedComm* **2021**, *2*, 569−586.
(17) Prasher, P.; Sharma, M. Mucoadhesive Nanoformulations and Their Potential for Combating Covid-19. *Nanomedicine* **2021**, *16*, 2497−2501.
(18) Bentley, K.; Stanton, R. J. Hydroxypropyl Methylcellulose-Based Nasal Sprays Effectively Inhibit in Vitro Sars-Cov-2 Infection and Spread. *Viruses* **2021**, *13*, 2345.
(19) Nambulli, S.; Xiang, Y.; Tilston-Lunel, N. L.; Rennick, L. J.; Sang, Z.; Klimstra, W. B.; Reed, D. S.; Crossland, N. A.; Shi, Y.; Duprex, W. P. Inhalable Nanobody (Pin-21) Prevents and Treats Sars-Cov-2 Infections in Syrian Hamsters at Ultra-Low Doses. *Sci. Adv.* **2021**, *7*, No. eabh0319.
(20) Schoof, M.; Faust, B.; Saunders, R. A.; Sangwan, S.; Rezelj, V.; Hoppe, N.; Boone, M.; Billesbolle, C. B.; Puchades, C.; Azumaya, C. M.; Kratochvil, H. T.; Zimanyi, M.; Deshpande, I.; Liang, J.; Dickinson, S.; Nguyen, H. C.; Chio, C. M.; Merz, G. E.; Thompson, M. C.; Diwanji, D.; Schaefer, K.; Anand, A. A.; Dobzinski, N.; Zha, B. S.; Simoneau, C. R.; Leon, K.; White, K. M.; Chio, U. S.; Gupta, M.; Jin, M.; Li, F.; Liu, Y.; Zhang, K.; Bulkley, D.; Sun, M.; Smith, A. M.; Rizo, A. N.; Moss, F.; Brilot, A. F.; Pourmal, S.; Trenker, R.; Pospiech, T.; Gupta, S.; Barsi-Rhyne, B.; Belyy, V.; Barile-Hill, A. W.; Nock, S.; Liu, Y.; Krogan, N. J.; Ralston, C. Y.; Swaney, D. L.; Garcia-Sastre, A.; Ott, M.; Vignuzzi, M.; Consortium, Q. S. B.; Walter, P.; Manglik, A.; et al. An Ultrapotent Synthetic Nanobody Neutralizes Sars-Cov-2 by Stabilizing Inactive Spike. *Science* **2020**, *370*, 1473−1479.
(21) Goscianska, J.; Freund, R.; Wuttke, S. Nanoscience Versus Viruses: The Sars-Cov-2 Case. *Adv. Funct. Mater.* **2021**, *32*, No. 2107826.
(22) Go, C. C.; Pandav, K.; Sanchez-Gonzalez, M. A.; Ferrer, G. Potential Role of Xylitol Plus Grapefruit Seed Extract Nasal Spray Solution in Covid-19: Case Series. *Cureus* **2020**, *12*, No. e11315.
(23) Li, Z.; Wang, Z.; Dinh, P. C.; Zhu, D.; Popowski, K. D.; Lutz, H.; Hu, S.; Lewis, M. G.; Cook, A.; Andersen, H.; Greenhouse, J.; Pessaint, L.; Lobo, L. J.; Cheng, K. Cell-Mimicking Nanodecoys Neutralize Sars-Cov-2 and Mitigate Lung Injury in a Non-Human Primate Model of Covid-19. *Nat. Nanotechnol.* **2021**, *16*, 942−951.
(24) Qin, M.; Cao, Z.; Wen, J.; Yu, Q.; Liu, C.; Wang, F.; Zhang, J.; Yang, F.; Li, Y.; Fishbein, G.; Yan, S.; Xu, B.; Hou, Y.; Ning, Z.; Nie, K.; Jiang, N.; Liu, Z.; Wu, J.; Yu, Y.; Li, H.; Zheng, H.; Li, J.; Jin, W.; Pang, S.; Wang, S.; Chen, J.; Gan, Z.; He, Z.; Lu, Y. An Antioxidant Enzyme Therapeutic for Covid-19. *Adv. Mater.* **2020**, *32*, No. 2004901.
(25) Frank, S.; Brown, S. M.; Capriotti, J. A.; Westover, J. B.; Pelletier, J. S.; Tessema, B. In Vitro Efficacy of a Povidone-Iodine Nasal Antiseptic for Rapid Inactivation of Sars-Cov-2. *Otolaryngol.−Head Neck Surg.* **2020**, *146*, 1054−1058.
(26) Edwards, D.; Hickey, A.; Batycky, R.; Griel, L.; Lipp, M.; Dehaan, W.; Clarke, R.; Hava, D.; Perry, J.; Laurenzi, B.; Curran, A. K.; Beddingfield, B. J.; Roy, C. J.; Devlin, T.; Langer, R. A New Natural Defense against Airborne Pathogens. *QRB Discovery* **2020**, *1*, No. e5.
(27) Edwards, D.; Salzman, J.; Devlin, T.; Langer, R. Nasal Calcium-Rich Salts for Cleaning Airborne Particles from the Airways of Essential Workers, Students, and a Family in Quarantine. *Mol. Front. J.* **2020**, *04*, 36−45.
(28) Burton, M. J.; Clarkson, J. E.; Goulao, B.; Glenny, A. M.; McBain, A. J.; Schilder, A. G.; Webster, K. E.; Worthington, H. V. Antimicrobial Mouthwashes (Gargling) and Nasal Sprays Administered to Patients with Suspected or Confirmed Covid-19 Infection to Improve Patient Outcomes and to Protect Healthcare Workers Treating Them. *Cochrane Database Syst. Rev.* **2020**, *9*, No. CD013627.
(29) Moakes, R. J. A.; Davies, S. P.; Stamataki, Z.; Grover, L. M. Formulation of a Composite Nasal Spray Enabling Enhanced Surface Coverage and Prophylaxis of Sars-Cov-2. *Adv. Mater.* **2021**, *33*, No. e2008304.
(30) Pilicheva, B.; Boyuklieva, R. Can the Nasal Cavity Help Tackle Covid-19? *Pharmaceutics* **2021**, *13*, 1612.
(31) Chavda, V. P.; Vora, L. K.; Pandya, A. K.; Patravale, V. B. Intranasal Vaccines for Sars-Cov-2: From Challenges to Potential in Covid-19 Management. *Drug Discovery Today* **2021**, *26*, 2619−2636.
(32) Casettari, L.; Illum, L. Chitosan in Nasal Delivery Systems for Therapeutic Drugs. *J. Controlled Release* **2014**, *190*, 189−200.
(33) Schütz, D.; Conzelmann, C.; Fois, G.; Gross, R.; Weil, T.; Wettstein, L.; Stenger, S.; Zelikin, A.; Hoffmann, T. K.; Frick, M.; Muller, J. A.; Munch, J. Carrageenan-Containing over-the-Counter Nasal and Oral Sprays Inhibit Sars-Cov-2 Infection of Airway Epithelial Cultures. *Am. J. Physiol.: Lung Cell. Mol. Physiol.* **2021**, *320*, L750−L756.
(34) Otto, D. P.; de Villiers, M. M. Layer-by-Layer Nanocoating of Antiviral Polysaccharides on Surfaces to Prevent Coronavirus Infections. *Molecules* **2020**, *25*, 3415.
(35) Cao, J.; Zaremba, O. T.; Lei, Q.; Ploetz, E.; Wuttke, S.; Zhu, W. Artificial Bioaugmentation of Biomacromolecules and Living Organisms for Biomedical Applications. *ACS Nano* **2021**, *15*, 3900−3926.
(36) Zhu, W.; Guo, J.; Amini, S.; Ju, Y.; Agola, J. O.; Zimpel, A.; Shang, J.; Noureddine, A.; Caruso, F.; Wuttke, S.; Croissant, J. G.; Brinker, C. J. Supracells: Living Mammalian Cells Protected within Functional Modular Nanoparticle-Based Exoskeletons. *Adv. Mater.* **2019**, *31*, No. e1900545.
(37) Zhu, W.; Guo, J.; Agola, J. O.; Croissant, J. G.; Wang, Z.; Shang, J.; Coker, E.; Motevalli, B.; Zimpel, A.; Wuttke, S.; Brinker, C. J. Metal-Organic Framework Nanoparticle-Assisted Cryopreservation of Red Blood Cells. *J. Am. Chem. Soc.* **2019**, *141*, 7789−7796.
(38) Guo, J.; Yu, Y.; Zhu, W.; Serda, R. E.; Franco, S.; Wang, L.; Lei, Q.; Agola, J. O.; Noureddine, A.; Ploetz, E.; Wuttke, S.; Brinker, C. J. Modular Assembly of Red Blood Cell Superstructures from Metal−Organic Framework Nanoparticle-Based Building Blocks. *Adv. Funct. Mater.* **2020**, *31*, No. 2005935.
(39) Liu, G.; Li, L.; Huo, D.; Li, Y.; Wu, Y.; Zeng, L.; Cheng, P.; Xing, M.; Zeng, W.; Zhu, C. A Vegf Delivery System Targeting Mi

https://doi.org/10.1021/acsami.2c03442
ACS Appl. Mater. Interfaces XXXX, XXX, XXX−XXX

Improves Angiogenesis and Cardiac Function Based on the Tropism of Mscs and Layer-by-Layer Self-Assembly. *Biomaterials* **2017**, *127*, 117−131.
(40) Jaber, N.; Al-Remawi, M.; Al-Akayleh, F.; Al-Muhtaseb, N.; Al-Adham, I. S. I.; Collier, P. J. A Review of the Antiviral Activity of Chitosan, Including Patented Applications and Its Potential Use against Covid-19. *J. Appl. Microbiol.* **2022**, *132*, 41−58.
(41) Serrano-Aroca, Á.; Ferrandis-Montesinos, M.; Wang, R. Antiviral Properties of Alginate-Based Biomaterials: Promising Antiviral Agents against Sars-Cov-2. *ACS Appl. Bio Mater.* **2021**, *4*, 5897−5907.
(42) Cano-Vicent, A.; Hashimoto, R.; Takayama, K.; Serrano-Aroca, A. Biocompatible Films of Calcium Alginate Inactivate Enveloped Viruses Such as Sars-Cov-2. *Polymers* **2022**, *14*, 1483.
(43) Umar, Y.; Al-Batty, S.; Rahman, H.; Ashwaq, O.; Sarief, A.; Sadique, Z.; Sreekumar, P. A.; Haque, S. K. M. Polymeric Materials as Potential Inhibitors against Sars-Cov-2. *J. Polym. Environ.* **2021**, 1−20.
(44) Ryu, G.; Shin, H. W. Sars-Cov-2 Infection of Airway Epithelial Cells. *Immune Network* **2021**, *21*, No. e3.
(45) Gao, W.; Li, L.; Wang, Y.; Zhang, S.; Adcock, I. M.; Barnes, P. J.; Huang, M.; Yao, X. Bronchial Epithelial Cells: The Key Effector Cells in the Pathogenesis of Chronic Obstructive Pulmonary Disease? *Respirology* **2015**, *20*, 722−729.
(46) Wang, P.; Luo, R.; Zhang, M.; Wang, Y.; Song, T.; Tao, T.; Li, Z.; Jin, L.; Zheng, H.; Chen, W.; Zhao, M.; Zheng, Y.; Qin, J. A Cross-Talk between Epithelium and Endothelium Mediates Human Alveolar-Capillary Injury During Sars-Cov-2 Infection. *Cell Death Dis.* **2020**, *11*, No. 1042.
(47) Mygind, N.; Dahl, R. Anatomy, Physiology and Function of the Nasal Cavities in Health and Disease. *Adv. Drug Delivery Rev.* **1998**, *29*, 3−12.
(48) Tang, Z.; Zang, N.; Fu, Y.; Ye, Z.; Chen, S.; Mo, S.; Ren, L.; Liu, E. Hmgb1 Mediates Hadv-7 Infection-Induced Pulmonary Inflammation in Mice. *Biochem. Biophys. Res. Commun.* **2018**, *501*, 1−8.
(49) Kajon, A. E.; Gigliotti, A. P.; Harrod, K. S. Acute Inflammatory Response and Remodeling of Airway Epithelium after Subspecies B1 Human Adenovirus Infection of the Mouse Lower Respiratory Tract. *J. Med. Virol.* **2003**, *71*, 233−244.
(50) Prince, G. A.; Porter, D. D.; Jenson, A. B.; Horswood, R. L.; Chanock, R. M.; Ginsberg, H. S. Pathogenesis of Adenovirus Type 5 Pneumonia in Cotton Rats (Sigmodon Hispidus). *J. Virol.* **1993**, *67*, 101−111.
(51) Barber, G. N. Host Defense, Viruses and Apoptosis. *Cell Death Differ.* **2001**, *8*, 113−126.
(52) Arakawa, H.; Kohno, T.; Hiki, T.; Kaji, Y. Ct Pulmonary Angiography and Ct Venography: Factors Associated with Vessel Enhancement. *AJR, Am. J. Roentgenol.* **2007**, *189*, 156−161.

https://doi.org/10.1021/acsami.2c03442
ACS Appl. Mater. Interfaces XXXX, XXX, XXX−XXX